



HYDROELASTIC VIBRATION OF CIRCULAR PLATES

M. K. KWAK

*Department of Mechanical Engineering, Dongguk University, 26 Pil-Dong 3-Ga,
Joong-Gu, Seoul 100-715, Korea*

(Received 6 February 1996, and in final form 14 August 1996)

This paper is concerned with the virtual mass effect due to the presence of water on the natural frequencies of circular plates which are placed into a hole of an infinite rigid wall with one side exposed to water. This classical problem was solved by Lamb, but he provided limited theoretical results. To obtain the complete theoretical results, the so-called non-dimensionalized added virtual mass incremental factors are obtained by employing the integral transformation technique in conjunction with the Fourier–Bessel series approach. It is found that the non-dimensionalized added virtual mass incremental factors for circular plates vibrating in an infinite rigid wall with one side exposed to water are larger than those for circular plates which rest on a free surface. This is due to the fact that the rigid wall constrains the motion of the water, thus resulting in an increase in the kinetic energy of the water. It is also observed that the effect of water on the natural frequencies generally decreases with order.

© 1997 Academic Press Limited

1. INTRODUCTION

It is generally known that the natural frequencies of structures which are in contact with water, or immersed in water, decrease significantly compared to their natural frequencies in air. This is due to the fact that the vibration of a structure in contact with water is transferred to the water motion and results in a discernible increase in the kinetic energy of the total system. This problem is referred to as the fluid–structure interaction problem. The first fluid–structure interaction problem stemmed from the classical problems solved by Lord Rayleigh [1] and Lamb [2]. They investigated the increase of inertia due to the presence of water and suggested the use of an approximate formula based on the so-called added virtual mass incremental (AVMI) factor, which is the ratio between the kinetic energy of the water and the kinetic energy of the structure. Lamb [2] calculated the change in the natural frequencies of a thin circular plate clamped along its boundary and placed in the aperture of an infinite rigid plane wall in contact with water. However, his initial studies were confined to fundamental modes of circular plates. This motivated the current investigation on the addressed problem.

Since Lamb initiated the study on the vibration of circular plates in contact with water, there have been numerous theoretical and experimental investigations on the vibration of circular plates in contact with water [3–9]. It is worthwhile to note that the problem solved by Kwak and Kim [7] and Kwak [8] is different from Lamb's original problem, since they considered the case of circular plates resting on free surface. They found that the non-dimensionalized added virtual mass incremental (NAVMI) factors for simply supported and clamped circular plates resting on a free surface are considerably lower than those obtained by Lamb [2] and Peake and Thurston [5], but the NAVMI factors for

free-edge circular plates resting on free surface are almost identical with those obtained by Lamb [2] and Peake and Thurston [5]. They concluded that this is due to the kinetic energy increase of water caused by the rigid wall condition. Thus, the boundary condition of the water domain plays an important role in fluid–structure interaction problems.

The advantage of the approximate formula is that the characteristics of the fluid–structure interaction problem can be understood qualitatively and they are easy to use. However, the NAVMI factors are available only for circular plates and rectangular plates. To solve a fluid–structure interaction problem that involves complex geometry of a structure and water domain, it is necessary to resort to finite element modelling of fluid (FFEM) or the boundary element method (BEM) in conjunction with finite element modelling of the structure. However, the use of the FFEM or the BEM requires enormous amounts of time on modelling and computation. As a result, it is difficult to obtain a qualitative measure of the water effect by those methods.

In this paper, an attempt is made to obtain the NAVMI factors for uniform circular plates having simply supported, clamped and free-edge boundary conditions and vibrating in contact with water, which is the problem solved by Lamb only for fundamental modes. Compared to the rigorous mathematical results obtained by Kwak and Kim [7] and Kwak [8] for the case of circular plates resting on free surface, theoretical results for circular plates placed into a hole of an infinite rigid wall with one side exposed to water are available only for a few lower modes which are expressed in terms of simple polynomials [2, 5]. In this paper, the solution is sought for higher modes which are exact eigenfunctions of the circular plate vibrating in air. To this end, the Fourier–Bessel series approach used by Tranton [10, 11] is employed to solve the boundary value problem; this proved to be effective for the hydroelastic problem of membranes [12].

It is found that the NAVMI factors obtained in this paper are larger than those obtained by Kwak [8], and that the NAVMI factors for the fundamental modes are in good agreement with those obtained by Lamb [2], McLachlan [4], and Peake and Thurston [5].

2. ADDED VIRTUAL MASS INCREMENTAL FACTOR

Consider a circular plate in contact with water (see Figure 1), where a and h represent the radius and the thickness of the circular plate respectively. As shown in Figure 1, the circular plate is placed into a hole in an infinite rigid wall, with one side exposed to water.

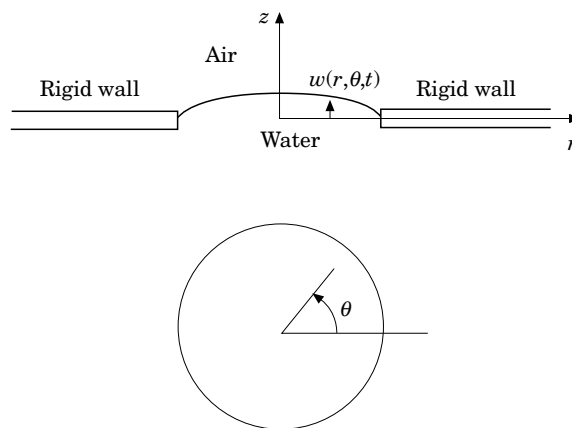


Figure 1. A circular plate in contact with water.

For simplicity, we assume the following for our analysis. (1) The wavelength is considerably smaller than the diameter of the plate, i.e., motion is small. (2) The water is incompressible, inviscid and irrotational. (3) The dynamic loading of water has an insignificant effect on mode shapes, so that there are few changes in the kinetic and potential energy of the circular plate in contact with water compared to those in air. (Espinosa and Juarez [6] and Amabili *et al.* [9] confirmed this assumption experimentally for the free-edge circular plates—unfortunately, this assumption has not been validated experimentally for simply supported and clamped circular plates). (4) The plate is thin elastic, and has uniform thickness and density, so that the small deflection theory of plates can be applied. (5) There are no internal losses, i.e., the system is conservative.

Rayleigh’s quotient is valid only for the fundamental mode. However, the third assumption enables the prediction of higher natural frequencies of plates in contact with water. Using Rayleigh’s quotient, one can write

$$f_a^2 \propto \left(\frac{V_p}{T_p^*} \right)_{air}, \quad f_w^2 \propto \left(\frac{V_p}{T_p^* + T_w^*} \right)_{water} \tag{1}$$

where f_a is the natural frequency of plates in air, f_w is the natural frequency of plates in contact with water, T_p^* and V_p represent the reference kinetic energy and the maximum potential energy of the circular plate respectively, and T_w^* represents the reference kinetic energy of water due to the motion of the circular plate. The relation between the reference and maximum kinetic energy can be written as [13]

$$T_{max} = T^* \omega^2, \tag{2}$$

where ω is the frequency (in rad/s).

Based on the third assumption, the following formula can be derived from equations (1):

$$f_w = \frac{f_a}{\sqrt{1 + \gamma}}, \tag{3}$$

where γ represents the added virtual mass incremental (AVMI) factor defined by the ratio of the kinetic energy of water due to the motion of the circular plate over the kinetic energy of the circular plate itself, i.e.,

$$\gamma = \frac{T_w^*}{T_p^*} = \Gamma (\rho_w a / \rho_p h) = \Gamma \beta, \tag{4}$$

where ρ_w is the density of water, ρ_p is the mass density of the circular plate, Γ is the non-dimensionalized added virtual mass incremental (NAVMI) factor, which is a function of mode shapes and boundary conditions, and $\beta = \rho_w a / \rho_p h$ is called a thickness correction factor. The objective of this paper is to compute Γ .

The differential equation of motion for the circular plate shown in Figure 1 without the presence of water can be written as

$$D_E \nabla^4 w(r, \theta, t) + \rho_p \frac{\partial^2 w(r, \theta, t)}{\partial t^2} = 0, \tag{5}$$

where $w(r, \theta, t)$ is the deflection of the plate and $D_E = Eh^3/12(1 - \nu^2)$ is the flexural rigidity, in which E is the Young’s modulus and ν is the Poisson ratio. By separation of variables and assuming harmonic motion, the solution of equation (5) is expressed as

$$w(r, \theta, t) = \sum_{s=0}^{\infty} \sum_{n=0}^{\infty} W_{sn}(r) \cos s\theta \sin \omega t, \quad (6)$$

where ω is a function of the dimensionless parameter λ_{sn} and

$$W_{sn}(r) = A_{sn} J_s(\lambda_{sn} r/a) + C_{sn} I_s(\lambda_{sn} r/a) \quad (7)$$

represents the eigenvector corresponding to specified nodal diameter and nodal circle, in which J_s and I_s are, respectively, the Bessel function of the first kind and the modified Bessel function of the first kind of order s . λ_{sn} (the eigenvalues), A_{sn} and C_{sn} are determined by applying the boundary conditions. The values are given by Leissa [14] for the clamped circular plates, by Leissa and Narita [15] for simply supported circular plates and by Itao and Crandall [16] for free-edge circular plates.

Next, consider the water domain with which the plate and the wall are in contact. The three-dimensional oscillatory flow in cylindrical co-ordinates can be described by the velocity potential

$$\Phi(r, \theta, z, t) = \phi(r, z) \cos s\theta \omega \cos \omega t, \quad (8)$$

where the spatial velocity potential, $\phi(r, z)$, satisfies the reduced form of the Laplace equation:

$$\nabla^2 \phi(r, z) = 0. \quad (9)$$

If one considers the plate and the rigid wall to be impermeable, the velocities of water and the plate particle in contact should be identical at the water-plate and water-wall interfaces:

$$\left. \frac{\partial \phi}{\partial z} \right|_{z=0} = \begin{cases} -W_{sn}(r), & 0 < r < a, \\ 0, & r > a. \end{cases} \quad (10)$$

In addition, the radiation condition requires that the disturbance attenuate as the distance from the plate becomes large:

$$\phi, \frac{\partial \phi}{\partial r}, \frac{\partial \phi}{\partial z} \rightarrow 0 \quad \text{as } r, z \rightarrow \infty. \quad (11)$$

Hence, the boundary value problem for a circular plate vibrating in contact with water can be written

$$\frac{\partial^2 \phi}{\partial r^2} + \frac{\partial \phi}{r \partial r} + \frac{\partial^2 \phi}{\partial z^2} - \frac{s^2}{r^2} \phi = 0, \quad (12)$$

$$\left. \frac{\partial \phi}{\partial z} \right|_{z=0} = \begin{cases} -W_{sn}(r), & 0 < r < a, \\ 0, & r > a, \end{cases} \quad (13)$$

$$\phi, \frac{\partial \phi}{\partial r}, \frac{\partial \phi}{\partial z} \rightarrow 0 \quad \text{as } r, z \rightarrow \infty. \quad (14)$$

The boundary value problem consisting of partial differential equation (12) and boundary conditions (13) and (14) is conveniently handled by means of an integral transform. Considering the cylindrical co-ordinate system, the obvious choice is the Hankel transformation [17], which is denoted by

$$\bar{\phi}_h(\xi, z) = \int_0^\infty r\phi(r, z)J_s(\xi r) dr. \tag{15}$$

Moreover, one can derive the following relation by integrating by parts:

$$\int_0^\infty r \left(\frac{\partial^2 \phi}{\partial r^2} + \frac{\partial \phi}{r \partial r} - \frac{s^2}{r^2} \phi \right) J_s(\xi r) dr = -\xi^2 \bar{\phi}_h(\xi, z). \tag{16}$$

Multiplying equation (12) by $rJ_s(\xi r) dr$, integrating over the entire radius, and using equations (15) and (16), the partial differential equation, equation (12), is reduced to the ordinary differential equation:

$$d^2 \bar{\phi}_h / dz^2 - \xi^2 \bar{\phi}_h = 0, \tag{17}$$

From the boundary condition (14), we conclude that the solution of equation (17) should consist of the attenuating part only. Therefore, the solution of equation (17) has the form of

$$\bar{\phi}_h(\xi, z) = B(\xi) e^{-\xi z}. \tag{18}$$

Using the inversion formula of the Hankel transformation and equation (18), we obtain

$$\phi(r, z) = \int_0^\infty \xi \bar{\phi}_h(\xi, z) J_s(\xi r) d\xi = \int_0^\infty \xi B(\xi) e^{-\xi z} J_s(\xi r) d\xi. \tag{19}$$

Inserting equation (19) into the boundary condition (13) yields

$$\int_0^\infty \xi^2 B(\xi) J_s(\xi r) d\xi = \begin{cases} -W_{sn}(r), & 0 < r < a, \\ 0, & r > a. \end{cases} \tag{20}$$

Now, the variables can be non-dimensionalized by the introduction of the following new variables:

$$\rho = r/a, \quad \eta = a\xi, \quad A(\eta) = \eta^2 B(\eta), \quad F_{sn}(\rho) = a^3 W_{sn}(\rho). \tag{21}$$

Hence, the integral equation (20) can be cast into the following form of an integral equation:

$$\int_0^\infty A(\eta) J_s(\eta \rho) d\eta = \begin{cases} -F_{sn}(\rho), & 0 < \rho < 1, \\ 0, & \rho > 1. \end{cases} \tag{22}$$

If the integral equation (22) is solved for $A(\eta)$, then $B(\eta)$ can be derived using equation (21) and $\phi(r, z)$ using the inversion formula (19).

The exact solution for the above integral equation exists only for the simple case of $F_{sn}(\rho)$, i.e., when the mode shape is expressed in terms of simple polynomials [2, 4, 5]. For the mode shapes considered in this paper which consist of Bessel functions, the solution has never been obtained. In this paper, we propose the use of Fourier–Bessel series for the above integral equation, based on the approach used by Tranton [10, 11]. First, consider the following integral. It can be readily obtained from mathematical tables [18] that

$$\int_0^{\infty} J_{s+2m+1}(\eta) J_s(\rho\eta) d\eta = \begin{cases} \rho^s P_n^{(s,0)}(1-2\rho^2), & 0 < \rho < 1, \\ 0, & \rho > 1. \end{cases} \quad (23)$$

where the $P_n^{(s,0)}(x)$ represent Jacobi's polynomials. Hence, if we express $A(\eta)$ in terms of the following Bessel series,

$$A(\eta) = \sum_{m=0}^{\infty} a_m J_{s+2m+1}(\eta), \quad (24)$$

then equation (22) is automatically satisfied for $\rho > 1$. Also, if we apply Hankel's inversion formula to the integral equation (23), then we obtain

$$\eta^{-1} J_{s+2m+1}(\eta) = \int_0^1 \rho^{s+1} P_n^{(s,0)}(1-2\rho^2) J_s(\eta\rho) d\rho. \quad (25)$$

Equation (25) will prove its effectiveness when dealing with integrals involving Jacobi's polynomials and Bessel functions.

Inserting equation (24) into equation (22), multiplying it by $\rho^{s+1} P_l^{(s,0)}(1-2\rho^2)$ and integrating with respect to ρ between 0 and 1, one obtains

$$\begin{aligned} \sum_{m=0}^{\infty} a_m \int_0^{\infty} \int_0^1 J_{s+2m+1}(\eta) \rho^{s+1} P_l^{(s,0)}(1-2\rho^2) J_s(\eta\rho) d\rho d\eta \\ = - \int_0^1 F_{sn}(\rho) \rho^{s+1} P_l^{(s,0)}(1-2\rho^2) d\rho. \end{aligned} \quad (26)$$

Interchanging the order of integration and using the result of equation (25) yields

$$\sum_{m=0}^{\infty} a_m \int_0^{\infty} \eta^{-1} J_{s+2m+1}(\eta) J_{s+2l+1}(\eta) d\eta = E_{sn}^l \quad (27)$$

where

$$E_{sn}^l = -a^3 \int_0^1 W_{sn}(\rho) \rho^{s+1} P_l^{(s,0)}(1-2\rho^2) d\rho. \quad (28)$$

It can be obtained from mathematical tables [18] that the left side integral of equation (27) results in the following relation:

$$\int_0^{\infty} \eta^{-1} J_{s+2m+1}(\eta) J_{s+2l+1}(\eta) d\eta = \begin{cases} (2s+4m+2)^{-1}, & m=l, \\ 0, & m \neq l. \end{cases} \quad (29)$$

Moreover, recalling equation (7), it becomes evident that the evaluation of F_{sn}^l requires the following integration results, which can be derived from equation (25):

$$\int_0^1 \rho^{s+1} P_l^{(s,0)}(1-2\rho^2) J_s(\lambda\rho) d\rho = \frac{J_{s+2l+1}(\lambda)}{\lambda}, \quad (30)$$

$$\int_0^1 \rho^{s+1} P_l^{(s,0)}(1-2\rho^2) I_s(\lambda\rho) d\rho = \frac{I_{s+2l+1}(\lambda)}{\lambda}. \tag{31}$$

Therefore, inserting equation (7) into equation (28) and using equations (30) and (31), we can obtain

$$E_{sn}^l = \frac{-a^3}{\lambda_{sn}} [A_{sn} J_{s+2l+1}(\lambda_{sn}) + (-1)^l C_{sn} I_{s+2l+1}(\lambda_{sn})]. \tag{32}$$

Combining the result of equations (29) and (32), we can conclude that the coefficients of the Bessel series have the following form:

$$a_m = \frac{-a^3(2s+4m+2)}{\lambda_{sn}} [A_{sn} J_{s+2m+1}(\lambda_{sn}) + (-1)^m C_{sn} I_{s+2m+1}(\lambda_{sn})] \tag{33}$$

Let us compute the velocity potential at the water-plate interface, which can be written as

$$\phi(\rho, 0) = \frac{1}{a^2} \int_0^\infty \eta^{-1} A(\eta) J_s(\rho\eta) d\eta. \tag{34}$$

Letting $a_m^* = -a_m/a^3$, inserting equation (24) into equation (34) and using mathematical tables [18], one can obtain

$$\begin{aligned} \phi(\rho, 0) &= -a \sum_{m=0}^\infty \frac{a_m^* \rho^s \Gamma(s+m+\frac{1}{2})}{2\Gamma(m+\frac{3}{2})\Gamma(s+1)} {}_2F_1(s+m+\frac{1}{2}, -m-\frac{1}{2}; s+1, \rho^2), \\ &0 < \rho < 1, \end{aligned} \tag{35}$$

where ${}_2F_1(a, b; c, x)$ represents the hypergeometric function. Note that equation (35) is valid for $0 < \rho < 1$. The potential for $\rho > 1$ can be obtained, but it is not necessary for computation of the kinetic energy thus omitted.

The reference kinetic energy of the water can be written as

$$\begin{aligned} T_w^* &= -\frac{1}{2}\rho_w \int_0^{2\pi} \int_0^\infty \frac{\partial\phi(r, 0)}{\partial z} \phi(r, 0) r dr \cos^2 s\theta d\theta \\ &= -\frac{1}{2}\rho_w a^2 D_\theta \int_0^1 W_{sn}(\rho) \phi(\rho, 0) \rho d\rho, \end{aligned} \tag{36}$$

where

$$D_\theta = \begin{cases} 2\pi, & \text{for } s = 0, \\ \pi, & \text{for } s > 0. \end{cases} \tag{37}$$

Inserting equations (7) and (35) into equation (36), one obtains

$$\begin{aligned} T_w^* &= -\frac{1}{2}\rho_w a^3 D_\theta \sum_{m=0}^\infty \frac{a_m^* \Gamma(s+m+\frac{1}{2})}{2\Gamma(m+\frac{3}{2})\Gamma(s+1)} \\ &\times \int_0^1 W_{sn}(\rho) {}_2F_1(s+m+\frac{1}{2}, -m-\frac{1}{2}; s+1, \rho^2) \rho^{s+1} d\rho. \end{aligned} \tag{38}$$

TABLE 1

 Γ_{sn} for the simply supported case ($\nu = 0.3$)

n	$s = 0$	$s = 1$	$s = 2$	$s = 3$	$s = 4$	$s = 5$
0	0.75539	0.33225	0.22675	0.17521	0.14389	0.12259
1	0.25680	0.16951	0.13390	0.11232	0.09741	0.08634
2	0.15041	0.11321	0.09528	0.08327	0.07438	0.06744
3	0.10513	0.08469	0.07392	0.06625	0.06032	0.05553
4	0.08040	0.06751	0.06034	0.05502	0.05077	0.04724
5	0.06487	0.05597	0.05077	0.04672	0.04333	0.04037

Note that T_w^* is the reference kinetic energy of water loaded on one side of the circular plate. If the circular plate is loaded on both sides, the expression should be multiplied by 2.

The reference kinetic energy of the plate can be written as

$$T_p^* = \frac{1}{2} \rho_p h a^2 D_0 \int_0^1 W_{sn}^2 \rho \, d\rho. \quad (39)$$

If we choose A_{sn} and C_{sn} which satisfy $\int_0^1 W_{sn}^2 \rho \, d\rho = 1$, then the non-dimensionalized added virtual mass incremental factor, Γ_{sn} , based on equation (4), can be expressed as

$$\Gamma_{sn} = \sum_{m=0}^{\infty} \frac{a_m^* \Gamma(s+m+\frac{1}{2})}{2\Gamma(m+\frac{3}{2})\Gamma(s+1)} \int_0^1 W_{sn}(\rho) {}_2F_1(s+m+\frac{1}{2}, -m-\frac{1}{2}; s+1, \rho^2) \rho^{s+1} \, d\rho. \quad (40)$$

Unfortunately, the integral in equation (40) does not render a closed form expression. Thus, it is necessary to resort to the numerical integration technique for the evaluation of this integral.

The NAVMI factors, Γ_{sn} , obtained for simply supported, clamped and free-edge cases using equation (40), are tabulated up to $s = 5$ and $n = 5$ in Table 1. All of the numerical computations, including the integral shown in equation (40), were carried out using Mathematica [19]. It is found that up to $s = 5$ and $n = 5$, a ten-term series expansion was enough for the evaluation of $A(\eta)$, as the coefficient quickly converges to zero. As can be seen in Table 1, the NAVMI factors for the simply supported circular plate are somewhat higher than those of the clamped and free-edge circular plates, and the NAVMI factors for the free-edge circular plate have smaller values. The NAVMI factors for the simply supported and clamped circular plates are higher than those obtained by Kwak [8]. This is because the rigid wall condition creates an increase in the kinetic energy, since the rigid

TABLE 2

 Γ_{sn} for the clamped case

n	$s = 0$	$s = 1$	$s = 2$	$s = 3$	$s = 4$	$s = 5$
0	0.65381	0.29883	0.20834	0.16321	0.13535	0.11616
1	0.27613	0.16914	0.13123	0.10968	0.09496	0.08415
2	0.16513	0.11591	0.09565	0.08286	0.07368	0.06663
3	0.11541	0.08748	0.07494	0.06654	0.06026	0.05529
4	0.08786	0.06995	0.06146	0.05554	0.05096	0.04724
5	0.07043	0.05788	0.05155	0.04685	0.04299	0.03965

TABLE 3
 Γ_{sn} for the free-edge case ($\nu = 0.3$)

n	$s = 0$	$s = 1$	$s = 2$	$s = 3$	$s = 4$	$s = 5$
0	0.84883	0.33953	0.22326	0.16929	0.13755	0.11642
1	0.22935	0.17802	0.14287	0.11963	0.10326	0.09109
2	0.13979	0.11550	0.09891	0.08682	0.07759	0.07029
3	0.09769	0.08503	0.07556	0.06818	0.06223	0.05732
4	0.07498	0.06729	0.06125	0.05645	0.05269	0.04997
5	0.06041	0.05458	0.04900	0.04292	0.03542	0.02530

wall constrains the motion of the water. However, there is not much difference in NAVMI factors for the free-edge circular plate.

3. RIGID BODY MODES FOR FREE-EDGE CIRCULAR PLATES

There exist two rigid body modes for the free-edge circular plate, i.e., for $s = 0, 1$ and $n = 0$. Although Rayleigh [1], Lamb [2] and McLachlan [4] dealt with these cases, it would be worthwhile to prove this by using the current approach. Consider the following mode shapes for the rigid body motion:

$$W_{s,0} = \sqrt{2(s+1)}\rho^s, \quad s = 0, 1. \tag{41}$$

Inserting equation (41) into equation (28) results in

$$E_{sn}^l = \frac{-a^3 \sqrt{2(s+1)} \Gamma(s+l+1)}{\Gamma(s+1)\Gamma(l+1)} \int_0^1 \rho^{2s+1} P_l^{(s,0)}(1-2\rho^2) d\rho. \tag{42}$$

Using mathematical tables [18], equation (42) yields

$$E_{sn}^l = \begin{cases} -a^3/\sqrt{2(s+1)}, & l = 0, \\ 0, & l > 0. \end{cases} \tag{43}$$

Therefore there remains only one coefficient for $l = 0$, which is

$$a_0^* = \sqrt{2(s+1)}. \tag{44}$$

Inserting equation (41) into equation (40) and using equation (43), one can obtain

$$\Gamma_{s0} = \frac{(s+1)\Gamma(s+\frac{1}{2})}{\Gamma(\frac{3}{2})} \int_0^1 {}_2F_1(s+\frac{1}{2}, \frac{1}{2}; s+1, \rho^2)\rho^{2s+1} d\rho, \quad s = 0, 1. \tag{45}$$

Using the result of McLachlan's work [4] or the mathematical handbook [20] for the integral of the Hypergeometric function, one obtains

$$\Gamma_{s0} = \begin{cases} 8/3\pi, & s = 0, \\ 16/15\pi, & s = 1. \end{cases} \tag{46}$$

These results are identical to those obtained in references [1, 2, 4]. However, the vibration of free-edge circular plates placed in a baffle of a rigid wall is not realistic at all, as pointed out in references [7, 8].

4. DISCUSSION AND CONCLUSIONS

Water has a significant effect on the vibration characteristics of structures in contact with water. In general, natural frequencies in water are smaller than those in air because the total kinetic energy increases due to the presence of water. This phenomenon is often explained in terms of virtual mass increase. Assuming that the wet mode shapes are the same as the ones in air, it is possible to separate the coupled problem into independent boundary value problems. Then, the change of natural frequency due to the presence of water can be predicted by using the ratio between the kinetic energy of water and the kinetic energy of the circular plate, often called the added virtual mass incremental (AVMI) factor.

In this paper, the non-dimensionalized added virtual mass incremental (NAVMI) factors are obtained for the uniform circular plates vibrating in a hole of an infinite rigid wall. To this end, the Fourier–Bessel series expansion is employed to solve the integral equation obtained by the Hankel transformation.

It can be seen from Tables 1, 2, and 3 that the effect of water is dominant in the simply supported circular plates and less dominant in the free-edge circular plates. As pointed out earlier, the free-edge circular plates placed in a baffle are not realistic, but the computation was carried out to compare the results with Lamb's.

It is generally found that the NAVMI factor decreases as the number of nodal diameters and nodal circles increases, which has the same tendency as observed in the results obtained by Kwak [8]. For the specified nodal diameter, the NAVMI factor decreases with the number of nodal circles, and for the specified nodal circle, the NAVMI factor decreases as the number of nodal diameters increases. It is also found that the presence of water has the most significant effect on the fundamental mode of the circular plates regardless of the boundary condition. The NAVMI factors given in Tables 1, 2 and 3 can be directly applied to the determination of the natural frequencies of uniform circular plates in contact with water and placed into a hole in an infinite rigid wall. In the case of a circular plate resting on a free surface, one can use the results of Kwak [8]. It should be stressed again that the NAVMI factor should be doubled in the case of fully immersed circular plates.

ACKNOWLEDGMENT

This research was supported by the Korea Research Foundation through Young Investigator's Award 300-164.

REFERENCES

1. LORD RAYLEIGH 1877 *Theory of Sound* (two volumes), New York: Dover; second edition, 1945 re-issue.
2. H. LAMB 1920 *Proceedings of the Royal Society of London, Series A*, **98**, 205–216. On the vibrations of an elastic plate in contact with water.
3. J. H. POWELL and J. H. T. ROBERTS 1923 *Proceedings of the Physical Society (London)* **35**, 170–182. On the frequency of vibration of circular diaphragms.
4. N. W. MCLACHLAN 1932 *Proceedings of the Physical Society (London)* **44**, 546–555. The accession to inertia of flexible discs vibrating in a fluid.
5. W. H. PEAKE and E. G. THURSTON 1954 *Journal of the Acoustical Society of America* **26**, 166–168. The lowest resonant frequency of a water-loaded circular plate.
6. F. M. ESPINOSA and J. A. GALLEGO-JUAREZ 1984 *Journal of Sound and Vibration* **94**, 217–222. On the resonance frequencies of water-loaded circular plates.
7. M. K. KWAK and K. C. KIM 1991 *Journal of Sound and Vibration* **146**, 381–389. Axisymmetric vibration of circular plates in contact with fluid.

8. M. K. KWAK 1991 *Journal of Applied Mechanics* **58**, 480–483. Vibration of circular plates in contact with water.
9. M. AMABILI, G. DALPIZA and C. SANTOLINI 1994 *Proceedings of the 12th International Modal Analysis Conference, Honolulu, Hawaii*, 349–355. Free vibration of free-edge circular plates immersed in water.
10. C. J. TRANTON 1950 *Quarterly Journal of Mechanics and Applied Mathematics* **3**, 411–419. On some dual integral equations occurring in potential problems with axial symmetry.
11. C. J. TRANTON 1954 *Quarterly Journal of Mechanics and Applied Mathematics* **7**, 317–325. A further note on dual integral equations and an application to the diffraction of electromagnetic waves.
12. M. K. KWAK 1994 *Journal of Sound and Vibration* **178**, 688–690. Vibration of circular membranes in contact with fluid.
13. L. MEIROVITCH 1975 *Elements of vibration analysis*. New York: McGraw-Hill.
14. I. N. SNEDDON 1951 *Fourier Transforms*. New York: McGraw-Hill.
15. A. W. LEISSA 1969 *Vibration of plates*, NASA SP-160. Washington, D.C.: U.S. Government Printing Office.
16. A. W. LEISSA and Y. NARITA 1980 *Journal of Sound and Vibration* **70**, 221–229. Natural frequencies of simply-supported circular plates.
17. K. ITAO and S. H. CRANDALL 1979 *Journal of Applied Mechanics* **46**, 448–453. Natural modes and natural frequencies of uniform, Circular free-edge plates.
18. I. S. GRADSHTEYN and I. M. RYZHIK 1980 *Table of Integrals, Series and Products: Corrected and Enlarged Edition*. New York: Academic Press.
19. S. WOLFRAM 1988 *Mathematica: a System of Doing Mathematics by Computer*. Redwood City, CA: Addison-Wesley.
20. H. EXTON 1978 *Handbook of Hypergeometric Integrals, Theory, Applications, Tables, Computer Programs*. New York: Ellis Horwood.